International Journal of Chemical, Materials and Biomolecular Sciences
ISSN: 2415-6620
Vol:3, No:7, 2009

Surface Phonon Polariton in InAlGaN Quaternary Alloys

S. S. Ng, Z. Hassan, and H. Abu Hassan

***Abstract*—**III-nitride quaternary $In_xAl_yGa_{1-x-y}N$ alloys have experienced considerable interest as potential materials for optoelectronic applications. Despite these interesting applications and the extensive efforts to understand their fundamental properties, research on its fundamental surface property, i.e., surface phonon polariton (SPP) has not yet been reported. In fact, the SPP properties have been shown to provide application for some photonic devices. Hence, there is an absolute need for thorough studies on the SPP properties of this material. In this work, theoretical study on the SPP modes in InAlGaN quaternary alloys are reported. Attention is focus on the wurtzite (α-) structure $In_xAl_yGa_{1-x-y}N$ semi-crystal with different In composition, x ranging from 0 to 0.10 and constant Al composition, y = 0.06. The SPP modes are obtained through the theoretical simulation by means of anisotropy model. The characteristics of SP dispersion curves are discussed. Accessible results in terms of the experimental point of view are also given. Finally, the results revealed that the SPP mode of α-$In_xAl_yGa_{1-x-y}N$ semiconductors exhibits two-mode behavior.

***Keywords*—**III-nitride semiconductor, attenuated total reflection, quaternary alloy, surface phonon polariton.

I. Introduction

RECENTLY group-III nitride quaternary InAlGaN alloys have been found to be promising materials to overcome some shortfall of GaN epilayers, InGaN and AlGaN alloys [1]. This is because it allows the independent control of lattice constant and energy band gap. For example, by varying indium (In) and aluminum (Al) compositions x and y in $In_xAl_yGa_{1-x-y}N$, one can change the energy band gap while GaN-based lattice matched structures can be obtained [2]. In addition, it also has the potential to provide a better thermal match to GaN, which could be an important advantage in epitaxial growth and hence, giving much greater flexibility in the design of devices. In terms of devices applications, the InAlGaN can produce improved lattice matching to the cladding layer and better ultra-violet emission efficiency [3]. The emission efficiency of the quaternary alloys is about three times higher than the AlGaN ternary alloys with a comparable Al composition [1]. Besides that it offer a similar effect to that obtained in InGaN quantum wells [4]-[5].

Although some progress has been achieved in the fabrication of InAlGaN-based devices, many basic physical properties still remain unclear or unexplored. For instance, knowledge on the surface phonon polariton (SPP) mode, which is crucial for understanding the behavior of the coupling effect between the photon and surface phonon, has not yet been reported.

At present, the SPP properties of III-nitride binary and ternary semiconductors have been widely investigated [6]-[15]. Additionally, the SPP has been shown to provide application for some photonic devices [16]-[18]. Consequently, from both the fundamental physics point-of-view and the potential application of the nitride semiconductors, there is an absolute need for thorough study on the SPP properties.

In order to contribute to the understanding of the fundamental properties of this advanced material as well as the advancement of knowledge in the condensed matter, the SPP in the InAlGaN quaternary semiconductors are investigated. Attention is focused on the gallium-rich InAlGaN quaternary alloys because these alloys are lattice matched to GaN and have potential usage as GaN-based optoelectronic devices [3].

In this work, the SPP behaviors in wurtzite (α-) structure $In_xAl_yGa_{1-x-y}N$ semi-crystal with different In composition, x ranging from 0 to 0.10 and constant Al composition, y = 0.06 are investigated theoretically. The surface polariton (SP) dispersion relations are simulated based on an anisotropy model.

II. Theory

A SPP is resulting from the coupling of transverse magnetic (TM) infrared (IR) photon with a transverse-optic (TO) phonon. The frequency of this mode occurs in spectral regions where the sample's dielectric function is negative, which is between the TO and the longitudinal-optic (LO) phonon frequencies (TO < SPP < LO). Note that the coupling effects do not concern LO phonons because the LO phonons do not couple to TM photons.

In general, the SPP is a TM vibration mode which will travel along a direction perpendicular to the surface normal, as shown in Fig. 1(a). However, its amplitude is attenuated from

S. S. Ng is with the School of Physics, Universiti Sains Malaysia, 11800 USM, Penang, Malaysia. (phone: 604-653-3041; fax: 604-657-9150; e-mail: shashiong@usm.my).

Z. Hassan is with the School of Physics, Universiti Sains Malaysia, 11800 USM, Penang, Malaysia (e-mail: zai@usm.my).

H. Abu Hassan is with the School of Physics, Universiti Sains Malaysia, 11800 USM, Penang, Malaysia (e-mail: haslan@usm.my).

Supported by the Ministry of Higher Education Malaysia Fundamental Research Grant Scheme (FRGS Grant 203/PFIZIK/671162) and Universiti Sains Malaysia.

surface to bulk. Another unique feature of the SPP mode is that it can propagate through the forbidden band (interval between the TO and LO frequencies). This interval is often called the surface-mode window [19].

It is known that III-nitrides binary and ternary crystallize preferentially in hexagonal wurtzite (α-) structure. The cubic zinc-blende (β-) structure is a metastable one and observed only for heteroepitaxial layers on a cubic substrate (001)-oriented. Like its parents, InAlGaN also crystallizes in two polytypes, namely, hexagonal and cubic. However, the stable structure of InAlGaN is also hexagonal wurtzite structure. For this reason, the attention is focused on the α-InAlGaN and an anisotropy model is used to simulate its SP dispersion relations.

Let consider the SP dispersion relation based on the anisotropy model. Assume that the optic axis c of the α-InAlGaN crystal is parallel to the surface normal ($c_{\text{axis}} \parallel z$) and perpendicular to the propagation direction of the SP ($c_{\text{axis}} \perp x$), as shown in Fig. 1(a).

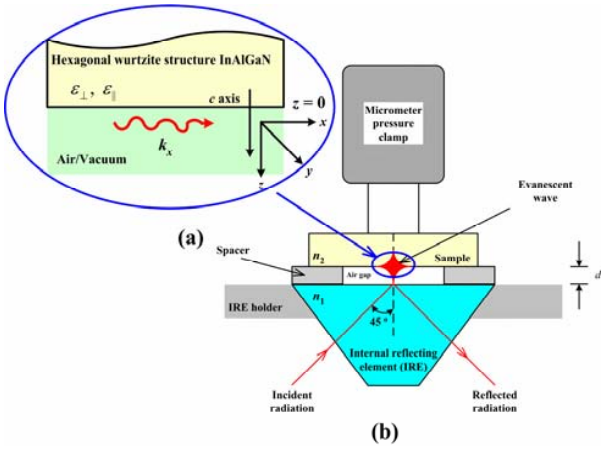

Fig. 1 (a) Geometry of the sample's orientation and coordinate system used and (b) schematic diagram of the ATR experiment setup

For optic axis c of the crystal parallel to the surface normal ($c_{\text{axis}} \parallel z$) and perpendicular to the propagation direction, the anisotropy model of the SP dispersion curves at the interface of α-InAlGaN semi-infinite crystal and vacuum is given by [20]:

$$\boldsymbol{k}_x(w) = \frac{w}{c}K(w) = \frac{w}{c}\left[\frac{\varepsilon_\parallel(w) - \varepsilon_\parallel(w)\varepsilon_\perp(w)}{1-\varepsilon_\perp(w)\varepsilon_\parallel(w)}\right]^{1/2}. \quad (1)$$

Here $\boldsymbol{k}_x(w)$ is the wave vector of the SP along the x direction and $K(w)$ is the dimensionless quantity; w and c are, respectively, the angular frequency of the SP and the velocity of light in vacuum (3×10^8 m s^{-1}). The $\varepsilon_{\parallel(\perp)}(w)$ is the dielectric function parallel (perpendicular) to the c-axis and is given by:

$$\varepsilon_{\parallel(\perp)}(w) = \varepsilon_{\infty,\parallel(\perp)}\left[\frac{w^2_{LO\parallel(\perp)} - w^2}{w^2_{TO\parallel(\perp)} - w^2}\right], \quad (2)$$

where $\varepsilon_{\infty,\parallel(\perp)}$ is the high-frequency dielectric constant parallel (perpendicular) to the c-axis. $w_{LO\parallel(\perp)}$ and $w_{TO\parallel(\perp)}$ are, respectively, the $LO_{\parallel(\perp)}$ and $TO_{\parallel(\perp)}$ zone centre phonons frequencies. The subscript $\parallel(\perp)$ refers to the parallel (perpendicular) vibration mode with respect to the optical axis c.

It should be pointed out that (2) is applied for binary system. For ternary alloy with the form of $A_xB_{1-x}C$, the expression for the $\varepsilon_{\parallel(\perp)}(w)$ is more complicated. The $\varepsilon_{\parallel(\perp)}(w)$ as a function of alloy composition x is given by [21]:

$$\varepsilon(A_xB_{1-x}C)_{\parallel,\perp} = x\varepsilon(AC)_{\parallel,\perp} + (1-x)\varepsilon(BC)_{\parallel,\perp}, \quad (3)$$

where $\varepsilon(AC)_{\parallel(\perp)}$ and $\varepsilon(BC)_{\parallel(\perp)}$ are, respectively, the dielectric constants parallel and perpendicular for AC and BC binary compounds.

The situation is even more complicated for the case of quaternary alloy. In a quaternary alloy of the $A_xB_yC_zD$ type, the quaternary alloy parameter $Q(x, y, z)$ is interpolated from the ternary parameters [22]. Analogously, the $\varepsilon_{\parallel(\perp)}(w)$ for the $In_xAl_yGa_{1-x-y}N$ quaternary alloy can be interpolated from the dielectric functions of ternary alloys, i.e., AlGaN, GaInN, and InAlN. Subsequently, the $\varepsilon_{\parallel(\perp)}(w)$ for the $In_xAl_yGa_{1-x-y}N$ as a function of alloys composition x, y, and z, can be written as:

$$\varepsilon(In_xAl_yGa_zN)_{\parallel(\perp)} = \frac{yz\varepsilon(Al_uGa_{1-u}N)_{\parallel(\perp)} + xz\varepsilon(Ga_vIn_{1-v}N)_{\parallel(\perp)} + xy\varepsilon(In_wAl_{1-w}N)_{\parallel(\perp)}}{xy+yz+zx}, \quad (4)$$

where $z = 1-x-y$, $u = \frac{1+y-z}{2}$, $v = \frac{1+z-x}{2}$, and $w = \frac{1+x-y}{2}$.

In this work, the SP dispersion curves for the α-$In_xAl_yGa_{1-x-y}N$ semi-crystal with different In composition, x ranging from 0 to 0.10 and constant Al composition, y = 0.06 are simulated by using (1) to (4). The parameters used to model the SP dispersion curves are obtained from [23]-[28] and listed in Table I.

III. Results and Discussion

Fig. 2 shows the theoretical SP dispersion curves for α-$In_xAl_yGa_{1-x-y}N$ semi-crystal with constant Al composition, y = 0.06, In composition, x = 0.02, 0.04, 0.06, 0.08, and 0.10. The light wave in vacuum ($\boldsymbol{k}_{\text{vac}}(w) = w/c$) and the light waves [$\boldsymbol{k}_p(w)$] in the attenuated total reflection (ATR) prism (will be discussed in detail later) are also shown in Fig. 2.

Conventionally, the SP dispersion curve is separated by the $\boldsymbol{k}_{\text{vac}}(w)$ line into two regions. However, only the region lies to the right of the $\boldsymbol{k}_{\text{vac}}(w)$ line is of great interest in this framework, because this region is a consequence of the TM IR photons and TO phonons coupling. In addition, this region is

TABLE I
PARAMETERS USED IN MODELING THE SURFACE POLARITON DISPERSION CURVES FOR WURTZITE (α-) STRUCTURE $In_xAl_yGa_{1-x-y}N$ SEMI-CRYSTAL WITH DIFFERENT In COMPOSITION, x RANGING FROM 0 TO 0.10 AND CONSTANT Al COMPOSITION, y = 0.06.

III-nitride	$w_{TO\parallel}$ (cm^{-1})	$w_{LO\parallel}$ (cm^{-1})	$\varepsilon_{\infty,\parallel}$	$w_{TO\perp}$ (cm^{-1})	$w_{LO\perp}$ (cm^{-1})	$\varepsilon_{\infty,\perp}$
InN	447[a]	586[a]	8.10[b]	476[a]	593[a]	8.34[b]
GaN	532[c]	734[c]	5.31[d]	559[c]	741[c]	5.14[d]
AlN	610[e]	891[e]	4.72[f]	670[e]	912[e]	4.53[f]

[a]Taken from Davydov *et al.* [23].
[b]Taken from Abbar *et al.* [24].
[c]Taken from Davydov *et al.*[25].
[d]Taken from Yu *et al.* [26].
[e]Taken from Haboek *et al.* [27].
[f]Taken from Persson *et al.* [28].

inaccessible by common IR reflectance or transmittance methods. Nonetheless, it is easily accessible by ATR method [29].

From Fig. 2, it can be found that the SP dispersion curves of the α-$In_xAl_yGa_{1-x-y}N$ have similar pattern to that of the α-$In_xGa_{1-x}N$ [10] and of the α-$Al_xGa_{1-x}N$ [13]. Namely, each SP dispersion curve can be divided into three branches, the upper (A), the middle (B), and the lower (C) branches. Among these branches, the middle branch B is of special interest, as it has the highest spectral strength (with larger k value). However, it should be pointed out here that the branch A in the SP dispersion curves of x = 0.05 and 0.10, as well as the branch C in the SP dispersion curve of x = 0.07 have higher spectral strength as compared to branch B. The reason for this phenomenon is still unclear at present. Future study needs to be done to understand this.

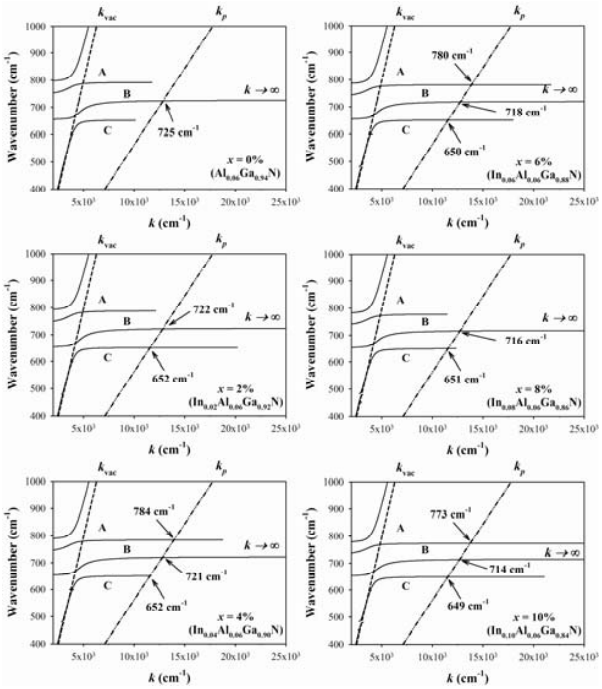

Fig. 2 Surface-polariton (SP) theoretical dispersion curves for wurtzite (α-) structure $In_xAl_yGa_{1-x-y}N$ semi-crystal with different In composition, x ranging from 0 to 0.10 and constant Al composition, y = 0.06. The vacuum light wave and the light wave in ATR crystal are indicated by dash line (---) and dash-dot-dot line (–··–), respectively. The intersections of the ATR crystal line and the branches of the SP dispersion curve correspond to the surface phonon polariton modes

Let consider the light wave [$\boldsymbol{k_p}(w)$] or the evanescent wave in the ATR prism and the relevant experimental information by ATR method. The wave vector $\boldsymbol{k_p}(w)$ is given by [20]:

$$\boldsymbol{k}_p(w) = \boldsymbol{k}_{\text{vac}}(w) n_p \sin\theta, \tag{5}$$

where n_p is the refractive index of the ATR prism, and θ is the internal angle of incidence in the prism. The $\boldsymbol{k_p}(w)$ is generated behind the base plane of the prism when the angle of the incident radiation exceeds the critical angle (θ_c) of prism. Coupling between the $\boldsymbol{k_p}(w)$ and the sample resulted the $\boldsymbol{k_x}(w)$ in which its propagation mode is in the x direction as shown in Fig. 1(a). When the wave vectors of the incident radiation and the SP are matched a resonance occurs. The frequency of this resonance is corresponds to the SPP mode. In principle, this mode is corresponds to the intersection of the SP dispersion curves with the $\boldsymbol{k_p}(w)$ line.

It is worth to mention that the Fig. 2, the $\boldsymbol{k_p}(w)$ lines are calculated using (5) with the values of n_p = 4.0 and θ = 45°, i.e., according to the common specifications for an ATR germanium prism [30]. The choice of this ATR prism depends upon its transmission spectral range where the SPP mode should occur. The typical experimental setup for the study of the SPP is shown in Fig. 1(b). For this experiment, incident radiation with TM polarization should be used as well in order to observe the SPP mode because it is a TM mode.

In Fig. 2, the intersection of the SP dispersion curves with the $\boldsymbol{k_p}(w)$ line is associated to the SPP mode of the $In_xAl_yGa_{1-x-y}N$. From Fig. 1, it is clearly seen that the number of intersecting points varies with the In composition. However, only the crossing points located on the branches B (CPsMB) and C (CPsLB) are considered as the SPP modes of the $In_xAl_yGa_{1-x-y}N$, i.e., based on the following criterions. It should be noted here that the SPP properties and behavior in the quaternary alloys have not yet been reported.

Basically, the SPP mode can be identified based on two criterions. Firstly, the SPP mode of the $In_xAl_yGa_{1-x-y}N$ ($0 < x \leq 0.10$) should be located at the frequency less than 725 cm^{-1}, i.e., the SPP mode for the $In_xAl_yGa_{1-x-y}N$ with x = 0. In fact, the incorporation of the In will shift the optical phonon modes [31] as well as the SPP mode [9] of the ternary compound toward the lower frequencies side. Consequently, it is supposed that the SPP mode for the $In_xAl_yGa_{1-x-y}N$ ($0 < x \leq 0.10$) should be lower than that of the $In_xAl_yGa_{1-x-y}N$ with x =

0. Lastly, the SPP mode of the $In_xAl_yGa_{1-x-y}N$ ($0 < x \leq 0.10$) should be shown In composition dependence. The variation magnitude of the SPP mode with In composition, however, is depends on a parameter known as bowing parameter. Based on these two criterions, it is suggests that both the CPsMB and the CPsLB can be considered as the SPP modes of the $In_xAl_yGa_{1-x-y}N$. Nevertheless, further investigation is needed to verify this result.

Fig. 3 shows the In composition dependence of the SPP modes for the $In_xAl_yGa_{1-x-y}N$ quaternary alloys. It is clearly seen that the frequency of the SPP modes gradually decreases as the x increases. However, it is found that the SPP mode located at branch B (SPP_B) is more In composition dependence (decreases faster) as compared to the SPP mode located at branch C (SPP_C). From Fig. 3, one can conclude that the behavior of the SPP mode in the $In_xAl_yGa_{1-x-y}N$ quaternary alloys can be classified as two-mode behavior.

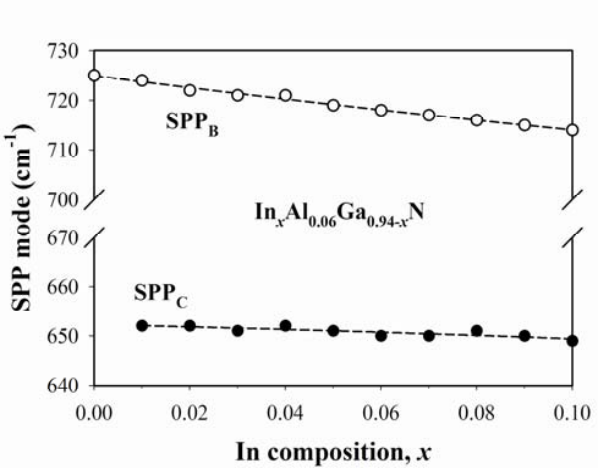

Fig. 3 Surface phonon polariton (SPP) modes as a function of In composition for the wurtzite (α-) structure $In_xAl_yGa_{1-x-y}N$ semi-crystal with different In composition, x ranging from 0 to 0.10 and constant Al composition, $y = 0.06$. The open and full circles correspond to the SPP modes located on the branches B (SPP_B) and C (SPP_C), respectively. The dashed lines represent the best fit of the nonlinear interpolation of the data. Note that the SPP theoretical data for $x = 0.01$, 0.03, 0.05, 0.07, and 0.09 are also included.

IV. Conclusion

In conclusion, the SPP mode of α-$In_xAl_yGa_{1-x-y}N$ semi-crystal with different In composition, x ranging from 0 to 0.10 and constant Al composition, $y = 0.06$ has been investigated theoretically be means of anisotropy model. The relevant experimental information by ATR method has also been discussed. The results showed that the SPP mode of α-$In_xAl_yGa_{1-x-y}N$ exhibits two-mode behaviors. Further work is on progress to fully clarify this result.

Acknowledgment

The support from Universiti Sains Malaysia is gratefully acknowledged.

References

[1] J. Li, K. B. Nam, K. H. Kim, J. Y. Lin, and H. X. Jiang, "Growth and optical properties of $In_xAl_yGa_{1-x-y}N$ quaternary alloys," *Appl. Phys. Lett.*, vol. 78, No. 1, pp. 61-63, 2001. [And references therein].

[2] F. G. McIntosh, K. S. Boutros, J. C. Roberts, S. M. Bedair, E. L. Piner, and N. A. El-Masry, "Growth and characterization of AlInGaN quaternary alloys," *Appl. Phys. Lett.*, vol. 68, No. 1, pp. 40-42, 1996.

[3] Y. A. Chang, S. H. Yen, T. C. Wang, H. C. Kuo, Y. K. Kuo, T. C. Lu, and S. C. Wang, **"**Experimental and theoretical analysis on ultraviolet 370 nm AlGaInN light-emitting diodes," *Semicond. Sci. Technol.*, vol. 21, No. 5, pp. 598-603, 2006.

[4] J. P. Liu , R. Q. Jin, J. C. Zhang, J. F. Wang, M. Wu, J. J. Zhu, D. G. Zhao, Y. T. Wang, and H. Yang, **"**Indium mole fraction effect on the structural and optical properties of quaternary AlInGaN epilayers," *J. Phys. D: Appl. Phys.*, vol. 37, No. 15, pp. 2060-2063, 2004. [And references therein].

[5] Y. Liu, T. Egawa, H. Ishikawa, B. J. Zhang, and M. S. Hao, "Influence of Growth Temperature on Quaternary AlInGaN Epilayers for Ultraviolet Emission Grown by Metalorganic Chemical Vapor Deposition," *Jpn. J. Appl. Phys.*, vol. 43, No. 5A, pp. 2414-2418, 2004. [And references therein].

[6] L. Zhang and J. J. Shi, "Surface phonon polariton modes of wurtzite structure $Al_xGa_{1-x}N$ thin film," *Phys. Status Solidi B*, vol. 246, No. 1, pp. 164-169, 2009.

[7] L. Zhang, "Surface phonon and confined phonon polaritons in wurtizte nitride thin-film structures," *Surf. Rev. Lett.*, vol. 15, No. 4, pp. 493-501, 2008.

[8] J. Bao and X. X. Liang, "Surface and interface phonon-polaritons in bilayer systems of polar ternary mixed crystals," *J. Appl. Phys.*, vol. 104, No. 3, pp. 033545-1 - 033545-7, 2008.

[9] S. S. Ng, Z. Hassan, and H. Abu Hassan, "Composition dependence of surface shonon polariton mode in wurtzite $In_xGa_{1-x}N$ ($0 \leq x \leq 1$) ternary alloy," *Chin. Phys. Lett.*, vol. 25, No. 12, pp. 4378-4380, 2008.

[10] S. S. Ng, Z. Hassan, and H. Abu Hassan, "Surface phonon polariton of wurtzite GaN thin film grown on *c*-plane sapphire substrate," *Solid State Commun.*, vol. 145, No. 11-12, pp. 535-538, 2008.

[11] M. D. He, L. L. Wang, W. Q. Huang, X. J. Wang, and B. S. Zou, "Surface phonon polaritons in a semi-infinite superlattice with a cap layer consisting of ternary crystal," *Phys. Lett. A*, vol. 360, No. 4-5, pp. 638-644, 2007.

[12] S. S. Ng, Z. Hassan, and H. Abu Hassan, "Surface phonon polariton mode of wurtzite structure $Al_xGa_{1-x}N$ ($0 \leq x \leq 1$) thin films," *Appl. Phys. Lett.*, vol. 91, No. 8, pp. 081909-1 - 081909-3, 2007.

[13] S. S. Ng, Z. Hassan, and H. Abu Hassan, "Experimental and theoretical studies of surface phonon polariton of AlN thin film," *Appl. Phys. Lett.*, vol. 90, No. 8, pp. 081902-1 - 081902-3, 2007.

[14] V. Y. Davydov, A. V. Subashiev, T. S. Cheng, C. T. Foxon, I. N. Goncharuk, A. N. Smirnovn, and R. V. Zolotareva, "Raman scattering by surface polaritons in cubic GaN epitaxial Layers," *Solid State Commun.*, vol. 104, No. 7, pp. 397-400, 1997.

[15] K. Torii, T. Koga, T. Sota, T. Azuhata, S. F. Chichibu, and S. Nakamura, "An attenuated-total-reflection study on the surface phonon-polariton in GaN," *J. Phys.: Condens. Matter*, vol. 12, No. 31, pp. 7041-7044, 2000.

[16] M. S. Anderson, "Enhanced infrared absorption with dielectric nanoparticles," *Appl. Phys. Lett.*, vol. 83, No. 14, pp. 2964-2966, 2003.

[17] J. J. Greffet, R. Carminati, K. Joulain, J. P. Mulet, S. Mainguy, and Y. Chen, "Coherent emission of light by thermal sources, *Nature*, vol. 416, pp. 61-64, 2002.

[18] A. J. Huber, N. Ocelic, R. Hillenbrand, "Local excitation and interference of surface phonon polaritons studied by near-field infrared microscopy," *J. Microscopy*, vol. 229, No. 3, pp. 389-395, 2008.

[19] M. G. Cottam and D. R. Tilley, *Introduction to surface and superlattice excitons*. New York: Cambridge University Press, 1989.

[20] D. N. Mirlin, "Surface Polaritons," in *Surface Polaritons*, V. M. Agranovich and D. L. Mills, Eds. Amsterdam: North-Holland, 1982, pp. 3-67.

[21] S. Adachi, *Optical properties of crystalline and amorphous semiconductors: Materials and fundamental principles*, Boston: Kluwer Academic, 1998, p. 38.

[22] C. K. Williams, T. H. Glisson, J. R. Hauser and M. A. Littlejohn, "Energy bandgap and lattice constant contours of III-V quaternary alloys

of the form $A_xB_yC_zD$ or $AB_xC_yD_z$," *J. Electron. Mater.*, vol. 7, no. 5, pp. 639-646, 1978.
[23] V. Y. Davydov, V. V. Emtsev, I. N. Goncharuk, A. N. Smirnov, V. D. Petrikov, V. V. Mamutin, V. A. Vekshin, S. V. Ivanov, M. B. Smirnov, and T. Inushima, "Experimental and theoretical studies of phonons in hexagonal InN," *Appl. Phys. Lett.*, vol. 75, No. 21, pp. 3297-3299, 1999.
[24] B. Abbar, B. Bouhafs, H. Aourag, G. Nouet, and P. Ruterana, "First-principles calculations of optical properties of AlN, GaN, and InN compounds under hydrostatic pressure," *Phys. Status Solidi B*, vol. 228, No. 2, pp. 457-460, 2001.
[25] V. Y. Davydov, Y. E. Kitaev, I. N. Goncharuk, A. N. Smirnov, J. Graul, O. Semchinova, D. Uffmann, M. B. Smirnov, A. P. Mirgorodsky, and R. A., Evarestov, "Phonon dispersion and Raman scattering in hexagonal GaN and AlN," *Phys. Rev. B*, vol. 58, No. 19, pp. 12899-12907, 1998.
[26] G. Yu, N. L. Rowell, and D. J. Lockwood, "Anisotropic infrared optical properties of GaN and sapphire," *J. Vac. Sci. Technol. A*, vol. 22, No. 4, pp. 1110-1114, 2004.
[27] U. Haboek, H. Siegle, A. Hoffmann, and C. Thomsen, "Lattice dynamics in GaN and AlN probed with first- and second-order Raman spectroscopy," *Phys. Status Solidi C*, vol. 0, No. 6, pp. 1710-1731, 2003.
[28] C. Persson, R. Ahyja, A. Ferreira da Silva, and B. Johansson, "First-principle calculations of optical properties of wurtzite AlN and GaN," *J. Cryst. Growth*, vol. 231, No. 3, 2001, pp. 407-414.
[29] A. Otto, "Spectroscopy of Surface Polaritons by Attenuated Total Reflection," in *Optical Properties of Solids: New Developments*, B. O. Seraphin, Ed. Norton-Holland: Amsterdam, 1976, p. 677.
[30] PIKE Technologies, Inc., "ATR-Theory and Applications," PIKE Technologies, Madison, Application Note, 2005.
[31] H. Grille, Ch. Schnittler, and F. Bechstedt, "Phonons in ternary group-III nitride alloys," *Phys. Rev. B*, vol. 61, No. 9, pp.6091-6105, 2000.